

Compact integrated optical sensor system

M. Wiki^{b,*}, H. Gao^{a,1}, M. Juvet^{1 a}, R.E. Kunz^{1 a}

^a CSEM Centre Suisse d'Electronique et de Microtechnique SA, Jaquet-Droz 1, CH-2007 Neuchatel, Switzerland

^b Division Optics, Unaxis Balzers Ltd., PO Box 1000 FL-9496 Balzers, Liechtenstein

Received 20 January 2000; received in revised form 19 September 2000; accepted 23 October 2000

Abstract

A compact integrated optical sensor system for a large variety of different (bio-) chemical applications using replicated sensor chips is described. Features of the refractometric system to be emphasized for practical applications include a high-resolution window that can be positioned within a wide measuring range, an in situ chip testing and characterization procedure, and on-chip referencing. As an application example, experimental results on refractometric measurements as well as on the suppression of non-specific binding are given. © 2001 Published by Elsevier Science B.V.

1. Introduction

Biosensors play an important role in diagnosis, medicine, process control and the development of new chemicals. These leads to a large demand of sensor systems that feature high resolution and serve as platform for a large variety of different (bio-) chemical applications. In addition, for medical applications using disposable sensor chips is essential.

Integrated optics (IO) is a well-known technique for directly measuring (bio-) chemical reactions at high resolution without the need of sample pre-treatment, such as labeling, prior to an experiment. Previously described IO sensors include sensors based on uniform grating couplers (BIOS-1²), chirped grating couplers (CGC) (Dübendorfer et al., 1998), surface plasmon resonance (Karlsson and Stahlberg, 1995; BIAcore³), resonant mirrors (Cush et al., 1993; IAsys⁴), and difference (Lukosz et al., 1996), Mach-Zehnder (Heideman et al., 1993) and Young (Brandenburg, 1997) interferome-

ters. Common to all systems is the measurement of changes in the effective refractive index N caused by the medium in contact with the waveguide. The systems mentioned allow to measure parameters such as the refractive index of liquids (Kempen and Kunz, 1994), humidity (Kunz, 1993), bio-chemical reactions, gas-concentrations (Tiefenthaler and Lukosz, 1984) and pH (Dübendorfer et al., 1998). To date, only few instruments are commercially available (BIOS-1,² BIAcore,³ IAsys⁴). They are generally rather bulky, and, in addition, the prices for the instruments and/or the sensor-chips are very high.

In this paper, a compact integrated optical sensor (CIOS) system based on the CGC sensing scheme (Kunz et al., 1994; Dübendorfer et al., 1998; Kunz, 1999) is presented. It is suitable for measuring changes in the effective refractive index at high resolution (Kunz et al., 1994; Dübendorfer et al., 1998) but the accessible measuring range is limited. By providing the system with an additional degree of freedom, a wide range for measuring the effective refractive index is obtained, which is important for practical applications. This approach enables the use of one single type of optical chip and a single system for a wide range of different applications. In addition, in situ chip testing and characterization procedures of the IO sensor chips allow to correct for errors occurring in the chip fabrication process. This feature in conjunction with replication techniques makes the sensor chips highly sensitive and low cost.

* Corresponding author. Tel.: +423-3884905; fax: +423-3885405.
E-mail addresses: max.wiki@unaxis.com (M. Wiki), rino.kunz@csem.ch (R.E. Kunz¹).

¹ Tel.: +41-32-7205165; fax: +41-32-7205740.

² BIOS-1 – Input grating coupler instrument, Artificial Sensing Instruments AG, Zurich, Switzerland.

³ BIAcore, BIAlite – Surface plasmon resonance biosensor, Biocore, Uppsala, Sweden.

⁴ IAsys – Resonant mirror biosensor system, Affinity Sensors, Cambridge, UK.

First, the sensing principle used in the CIOS system is described and some theoretical considerations that are relevant for practical applications are given. Then, the optical sensing scheme and a typical measurement procedure for exploiting the advantages of the CIOS system including chip testing and characterization are presented for a dual channel system. Finally, experimental results are presented in which the CIOS system is used as a refractometer and as a thin film sensor.

2. Sensing principle and theory

The sensing principle of the CIOS system is based on measuring the optical properties of a planar waveguide structure. It makes use of the evanescent field of a waveguide mode penetrating into the media adjacent to the waveguiding film. This is the reason why the surrounding media influences the light propagation velocity of the guided mode, described by the effective refractive index N . For sensing applications, intentionally caused changes in the cover medium are of particular interest. These changes in the cover can be determined by measuring the changes of the effective refractive index N of the waveguide structure.

A well-suited sensing scheme for measuring changes of the effective refractive index is the CGC scheme (Dübendorfer et al., 1998; Kunz, 1999). Since no mechanical movement is needed during the measurement, this scheme is advantageous for realizing miniature and high-resolution sensor systems. The schematic drawing of the sensor chip is given in Fig. 1. A single sensing unit consists of a pair of gratings G_i and G_o (Fig. 1(a) top view, Fig. 1(b) cross-section of the planar waveguide

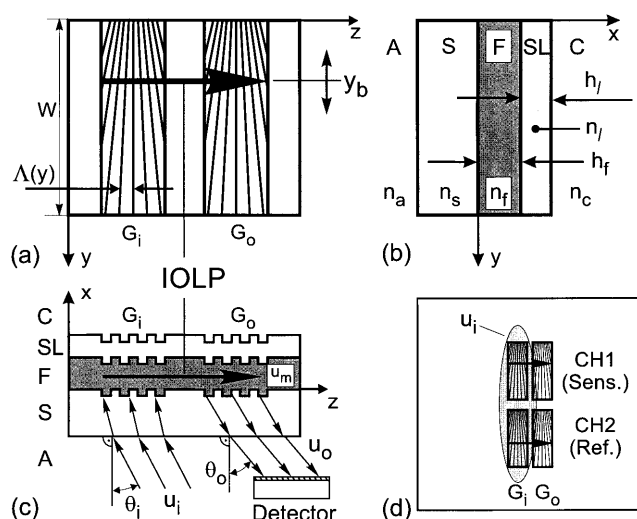


Fig. 1. CGC sensor for measuring changes in the effective refractive index. The layer structure surrounded by the ambient medium A is as follows: S – substrate; F – film; SL – sensing layer; C – cover; with the corresponding refractive indices (n_a , n_s , n_f , n_l , n_c) and thickness (h_f , h_l).

uide structure). For interrogating the sensor chip, the input grating G_i is illuminated with the collimated beam u_i of a laser with wavelength λ under a fixed angle of incidence θ_i , as shown in Fig. 1(c). At a certain position y_b on the grating where the linear varying grating period $A_i(y) = A_0 + g_A \times y$ fulfills the grating coupler condition (Kunz, 1993)

$$N = n_a \sin \theta_i + \frac{m_g \lambda}{A_i(y_b)}, \quad (1)$$

for the grating diffraction order m_g , a guided mode u_m , is excited with maximum intensity, forming an integrated optical light pointer (IOLP). A change of the effective refractive index will result in a change of the IOLP position y_b , which acts as an on-chip measuring variable. Its value is determined by coupling out the guided light via the output grating G_o . It is detected by observing the spatial intensity distribution of the emerging beam u_o .

The overall sensitivity of the sensor can be described by $\partial y_b / \partial M$ (Kunz et al., 1994), where M denotes the measurand, for example the cover refractive index n_c , the thickness h_l of a (bio-) chemical adlayer, the relative humidity, or the pH. For refractometric applications, the sensitivity can be represented as the product of two partial sensitivities, the primary and secondary transducer sensitivity, respectively.

$$\frac{\partial y_b}{\partial M} = \frac{\partial y_b}{\partial N} \times \frac{\partial N}{\partial M} \quad (2)$$

The primary sensitivity $\partial N / \partial M$ describes the efficiency of converting the measurand M into an optical parameter N describing the waveguide structure. The secondary sensitivity $\partial y_b / \partial N$ describes the sensitivity of the IO sensor for transducing changes in the effective refractive index into changes of the measuring variable, in our case the position y_b . To achieve a high-resolution sensor, both sensitivities have to be optimized. The primary sensitivity has to be optimized for the desired application. Ways to optimize the primary sensitivity include labeling the (bio-) molecules to be detected with mass labels (e.g. gold or dielectric particles) (Kubitschko et al., 1997), optimized sensing layer preparation (e.g. physical adsorbed layers or alternatively covalent bound sensing layers) and optimal parameters for sensing membranes (e.g. thickness and porosity) (Dübendorfer et al., 1998), among others. Optimization of the secondary sensitivity implies (Kunz et al., 1996) selection of appropriate transducer materials, the right polarization of the laser and ideal geometrical parameters for the planar waveguide sensor chip.

A drawback of the CGC sensor in practical applications is its limitation of the size w of the grating pads. The pad dimension limits the dynamic range for the maximal change of the IOLP position y_b . As a consequence, the measuring range for N and hence the

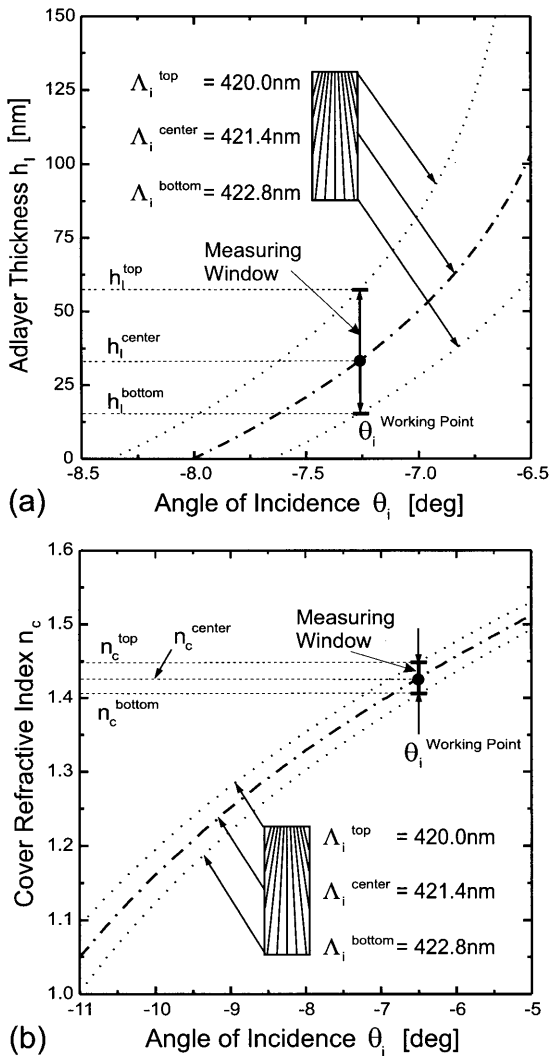


Fig. 2. Measuring window at different working points for measuring the thickness h_i of (a) a (bio-) chemical adlayer and (b) the cover refractive index n_c .

desired measurand M , is limited by the accessible measuring window. To overcome this drawback, the angle of incidence θ_i of the beam u_i is introduced as an additional degree of freedom. In the following, it will be shown how this angle can be used to set the working point of the sensor system. This approach leads to two

features that are essential for practical applications, at the same time. First, it allows to extend the measuring range by setting the working point, and second, it provides for a procedure to test and characterize the IO chips prior to a measurement. The latter will be described more in detail in a later section of this paper.

In Fig. 2 the extended measuring ranges, obtained by using the additional degree of freedom, are shown for two different applications, namely the use as a refractometer and as a thin film sensor. The calculations are based on a waveguide layer structure with refractive indices of (1.328/1.45/2.35/1.571) for $(n_c/n_i/n_r/n_s)$, respectively, a waveguide of thickness $h_r = 150 \text{ nm}$, a grating period of $\Lambda_i(y) = 420.0 \text{ nm} + 8.475 \times 10^{-7} \times y$ over a length of $w = 3.304 \text{ mm}$ and a TM_0 -polarized laser beam having wavelength of $\lambda = 785 \text{ nm}$. These parameters lead to a primary sensitivity for the sensor chip of $\partial y_b / \partial N = -266.5 \text{ mm}$. For the two major applications of the system, the secondary sensitivities are $\partial N / \partial n_c = 0.231$ for aqueous solutions as cover medium and $\partial N / \partial h_i = 4.591 \times 10^{-7} \text{ nm}^{-1}$ for a thin (bio-) chemical film growing on top of the sensor, respectively. The biosensor sensitivity was calculated assuming a layer thickness of $h_i = 3.0 \text{ nm}$. This thickness was chosen because it is a typical value occurring in practical measurements, where a “sensing layer” with about this thickness is most often immobilized on the chip surface before performing a measurement. Hence, the numerical results apply directly to typical biosensor measurements in real applications.

In Table 1, a list of primary and corresponding overall sensitivities for different measurands M is given. The primary sensitivities given show the changes of the effective refractive index N caused by changes of the surface mass coverage Γ , the adlayer thickness h_i , the refractive index n_i of the adlayer, and the cover refractive index n_c , respectively. Analogously, the overall sensitivity indicates the shift of the light pointer position y_b vs. changes of these measurands.

Results for the thin film sensor example are shown in Fig. 2(a). A working point set by choosing $\theta_i = -7.75^\circ$ results in a measuring window reaching from $h_i^{\text{bottom}} = 16.1$ to $h_i^{\text{top}} = 58.5 \text{ nm}$, corresponding to a span $\Delta h_i =$

Table 1
Primary and overall sensitivity of the CIOS-system (TM_0 -mode)^a

Measurand	M	Primary sensitivity		Overall sensitivity	
		$\partial N / \partial M$	Unit	$\partial y_b / \partial M$	Unit
Surface mass coverage	Γ	7.805×10^{-7}	mm^2/pg	-2.083×10^{-4}	mm^3/pg
Adlayer thickness	h_i	4.591×10^{-7}	nm^{-1}	-0.1225	mm/nm
Refractive index of adlayer	n_i	10.78×10^{-3}		-2.878	mm
Cover refractive index	n_c	0.231		-61.55	mm

^a Parameters used for the calculations: $n_c = 1.328$, $n_i = 1.45$; $h_i = 3.0 \text{ nm}$, $n_r = 2.35$, $h_r = 150 \text{ nm}$, $n_s = 1.571$, $\lambda = 785.0 \text{ nm}$, $\Lambda_i = 421.4 \text{ nm}$, $g_A = 8.47 \times 10^{-7}$, $\theta_i = -7.926^\circ$.

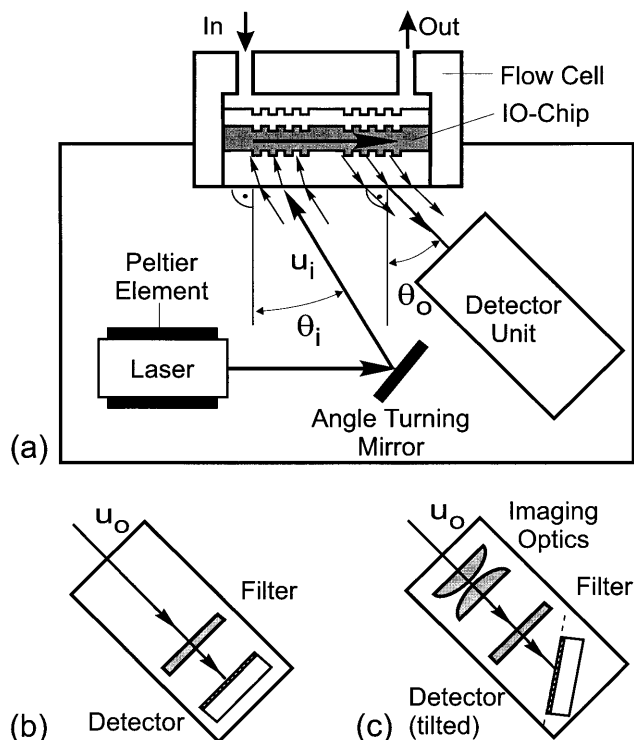


Fig. 3. (a) Schematic of the sensor system with two different detector units: (b) observation without and (c) with imaging optics.

42.4 nm for the high-resolution window, the effective refractive index span being $\Delta N = 0.0124$. For an increasing film thickness, an increase of the measuring window can be observed, originating from the limited penetration depth $\xi_c = 93.04$ nm of the evanescent field of the guided mode u_m into the cover medium.

Fig. 2(b) shows the corresponding results for an IO-refractometer. For a working point set by $\theta_i = -6.5^\circ$, the measuring window extends from $n_c^{\text{bottom}} = 1.405$ to $n_c^{\text{top}} = 1.449$, resulting in a cover refractive index span $\Delta n_c = 0.044$ (effective refractive index span $\Delta N = 0.0126$) for the high-resolution window. For the current sensor chips, the working point can be set anywhere within the wide range of $1.0 < n_c < 2.1$.

All considerations above have been made for one single channel. In practical applications, usually several channels are present at the same time to allow for on-chip-referencing or to specifically detect multiple kinds of measurands. The CGC sensing principle is well adapted for multiple single sensing units and can be arranged in an array pattern. As an example, the schematic of a dual channel arrangement, which was used in the experiments, is shown in Fig. 1(d). In this dual channel configuration, one channel can be addressed as sensing channel, the other as reference channel to allow on-chip referencing. This is essential to achieve high sensitivity and specificity (Dübendorfer and Kunz, 1996) as desired. In the experimental sec-

tion, an example demonstrating the improvement in specificity will be given.

3. Optical scheme and realization

A schematic drawing of the whole CIOS system for interrogating the CGC sensor chip is shown in Fig. 3. An angle turning mirror is used for varying the angle of incidence θ_i of a collimated laser beam u_i illuminating the input grating G_i of the IO sensor chip (Fig. 3(a)). As a result, the position y_b of the IOLP, coupled out by the grating G_o , varies on the detector according to the grating coupler resonance condition (Eq. (1)). This allows to set the working point of the system to the center of the grating region for a given experimental condition. It provides the user with a great flexibility for quickly adapting the system to a desired new or different application using one single type of gratings. On the detector side, two different schemes were used, both showed similar performance. The first one (Fig. 3(b)) directly detects the intensity distribution without the use of any optical components. This detection scheme was used for the (bio-) chemical applications described later in this paper. The second one (Fig. 3(c)) makes use of imaging optics using two lenses with a focal length of 40 mm. In order to correct for the tilted optical planes, Scheimpflug's rule (Scheimpflug, 1904) was applied. The advantage of this approach is that, in addition to the refractometric measurements, a visual inspection of the sensor chip is also feasible. This feature is useful to check for and identify disturbances such as (air) bubbles. Drawbacks are higher cost and a somewhat higher background intensity, which further depends on the material and construction of the cell body. The reasons to choose the version without imaging optics were the lower background and cost.

Fig. 4 shows a picture of the realized CIOS system (black box) together with a conventional flow injection analysis system for fluid supply. The chips can be mounted either in a flow cell or into cartridges for pipetting (not shown). As the light source, a laser diode (Röhm, RLD-78PP, 5 mW output power) emitting at a wavelength of $\lambda = 785$ nm was used. For keeping the wavelength at a constant value, the current and temperature of the laser diode were stabilized (Peltier element). A deflection mirror was mounted on a motorized mechanical unit to turn the beam around the pivot axis located at the input grating G_i . On the detector side, a commercial CCD camera (Sony, XC-77CE) was used for recording the intensity distribution of the IOLP.

4. Measurement procedure

A typical measurement procedure for the CIOS system for disposable sensor chips is shown in Fig. 5. In

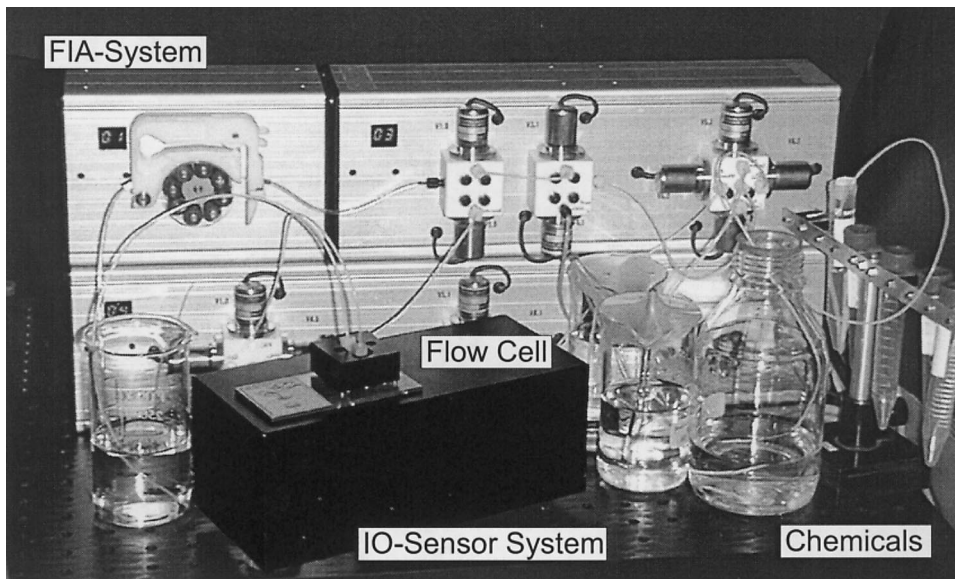


Fig. 4. Picture of the sensor system together with a fluidics arrangement.

an initialization step, the IO sensor chip is interrogated by scanning over the angle θ_i . This allows the user to determine the range of the measuring window on one hand and to characterize the chip on the other hand. Chips not fulfilling the specifications are rejected now in order to avoid false measurements. With this information about the sensor chip, the working point can be set to the desired position for the current application and enables generating the lookup-table before the measurement series are started. The lookup-table relates the incident angle θ_i and the measured IOLP position y_b . It thus contains information about defects, imperfections and non-linearity of the specific grating structure and the sensing layer, which is specific for each sensor chip and can be stored in a file for later use. After setting the working point and starting the measurement, the mirror is kept at the fixed position θ_i the CGC sensing principle does not require any moving parts during the measurement. The data of the current position y_b on the real sensor chip are acquired. After each measurement, or at the end of a complete series, the information of the lookup-table is used to eliminate the non-linearity characteristics of the specific sensor chip and derive a corrected IOLP position y_b^{corr} . The desired measurand M such as the cover refractive index n_c , the thickness h_1 of a chemical adlayer or the pH value can be calculated by applying the corresponding theoretical model.

5. Sensor chips: fabrication

For many applications, replicated low-cost sensor chips are essential. Two different kinds of replication techniques, namely hot-embossing and injection mold-

ing, have been used. Both techniques make use of a Ni-shim. The shim is fabricated by electroplating from an original microstructure produced by e-beam writing and dry etching techniques (Kunz et al., 1995).

The first fabrication method is based on hot-embossing the grating nano-structures into a polycarbonate foil (Röhm Europlex PC 99510, 250 μm thick, refractive index $n_s = 1.571$ at $\lambda = 785$ nm) by means of the Ni-shim. In the second method, the Ni-shim serves as master in an injection molding process for high volume

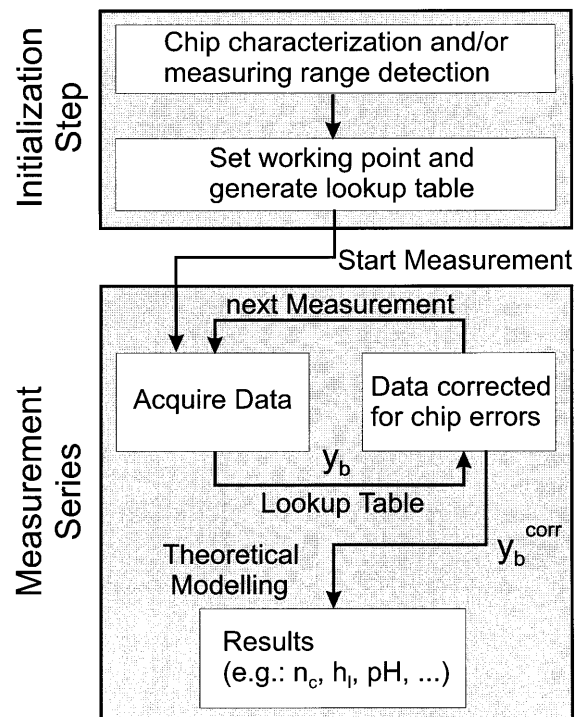


Fig. 5. Measurement procedure.

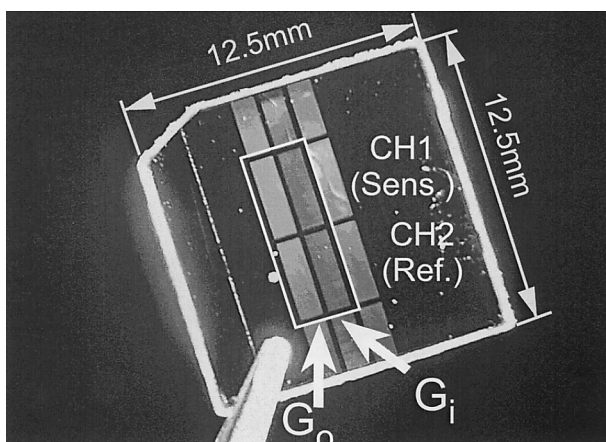


Fig. 6. Photograph of one single hot-embossed sensor chip.

production. Subsequent to replication, the pre-structured substrates were coated with TiO_2 by means of a low-temperature DC magnetron sputtering process forming a compact waveguide film ($n_f = 2.35$, $h_f = 150$ nm).

Fig. 6 shows a picture of a hot-embossed sensor chip with a size of 12.5×12.5 mm². Besides the two sensing channels CH1 and CH2 (also addressed as reference and sensing channels), with input gratings G_i and output gratings G_o , respectively, additional test structures can be seen. Using this kind of hot-embossed sensor chips, a resolution of $\delta N \approx \pm 1.0 \times 10^{-6}$ was demonstrated in a pH sensor application and other experiments including on-chip referencing, as reported earlier in (Dübendorfer and Kunz, 1998; Dübendorfer et al., 1998). The experiments reported in this paper were performed using hot-embossed sensor chips. The same performance was achieved with the injection-molded chips in other experiments.

6. Sensor chips: in situ chip testing and characterization

Quality testing of the chips immediately before the measurements markedly increases the reliability. In situ chip testing not only provides the possibility to correct for minor chip fabrication errors, but also to reject chips which might have been damaged due to improper storage or transportation (e.g. at excessive temperatures), or by any other inadequate handling.

During chip testing the intensity distribution at different angles θ_i is recorded. In Fig. 7 the intensity distribution of the IOLP is shown. For the angle of $\theta_i = -6.0945^\circ$ the IOLP of both channels CH1/CH2, as imagined onto the CCD detector, can be seen in Fig. 7(a). The corresponding normalized intensity projected onto one axis is shown in Fig. 7(b). The chip testing itself consists of a series of single measurements as can

be seen in Fig. 8. Fig. 8(a) shows a chip test record of a hot-embossed sensor chip for angles in the range of $6.1 < \theta_i < 6.6^\circ$ where the intensity distribution of single measurements (Fig. 7(a)) were arranged next to each other. This graph gives a good overview of the chip characteristics and contains information about defects, imperfections and non-linearity of the specific grating structure and sensing layer. For obtaining the lookup-table (Fig. 8(b)) the IOLP position y_b is extracted from the intensity distribution by fitting a Gaussian curve to each of the peaks.

It can be clearly seen in Fig. 8(b) that one channel (the lower channel on the graph) has a slight non-linearity and differs from an ideal linear relation. By knowing about this characteristic, which is specific for each sensor chip, one can easily corrected for this non-linearity. During the measurement, the information stored in the lookup-table is used to derive the corrected IOLP position y_b^{corr} from the measured position y_b .

7. Application: refractometer

One of the various application fields of the CIOS system is refractometric sensing. Fig. 9 shows an experiment for measuring the cover refractive index. Liquids having slightly different refractive indices were prepared by diluting D-glucose in H_2O . In the experiment, three different solutions with D-glucose of 14.20%, 14.28% and 14.85% (anhydrous solute weight per cent [g solute/100g solution]) were used. According to (CRC, 1989) and considering the dispersion of water (Schieber and Straub, 1990), the corresponding calculated refractive indices are 1.349729, 1.349855 and 1.350756, respectively, for a temperature of 20°C and a wavelength of

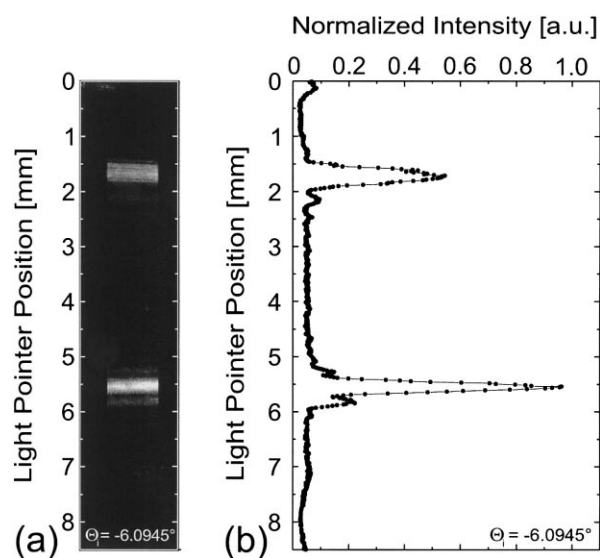


Fig. 7. Intensity distribution of the IOLP on the detector for (a) both channels (CH1/CH2 or sensing/reference, respectively) and (b) corresponding normalized intensity distribution.

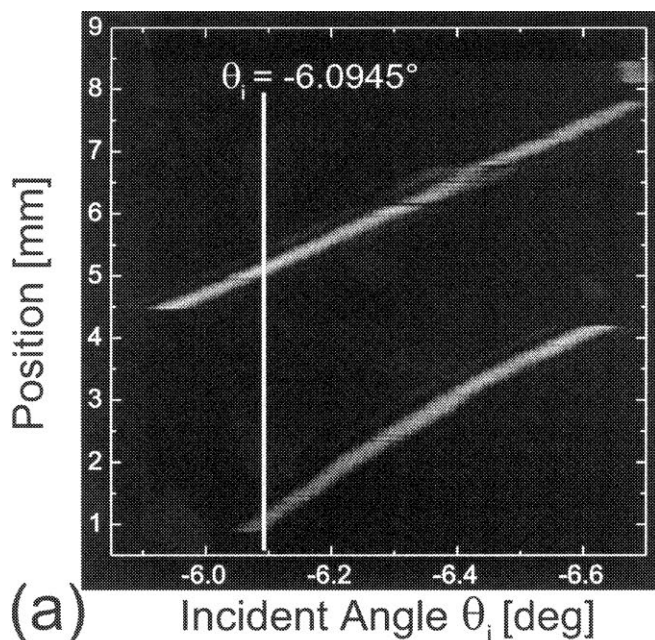
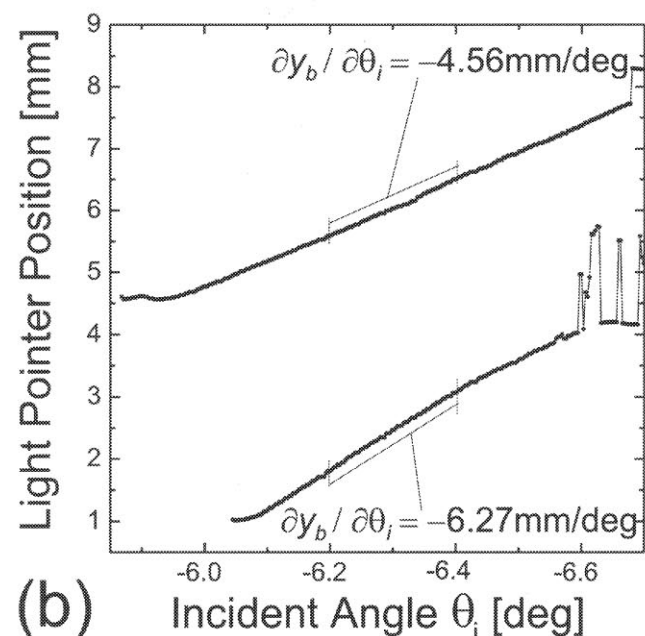
(a) Incident Angle θ_i [deg](b) Incident Angle θ_i [deg]

Fig. 8. (a) Intensity distribution of the IOLP for different angles of incidence and (b) characteristics for one specific sensor chip which is used as lookup-table to correct for non-linearity/defects of the sensor chip.

$\lambda = 785.0$ nm. By means of an FIA-system, the three liquids were delivered into the $5 \mu\text{l}$ flow-cell attached to the waveguide side of the IO sensor. The arrows in the sensorgram (Fig. 9) indicate the start of the switching between the different liquids. The results show that the measured refractive index differences Δn_c of the glucose solutions is in good agreement with the literature values of 1.26×10^{-4} and 10.27×10^{-4} , respectively.

8. Application: local surface passivation by dextran

A major application of CIOS is monitoring adsorption and binding of (bio-) molecules to surfaces. Here on-chip referencing becomes important: signal and reference channels can be recorded simultaneously.

The experiment detailed below exemplifies the suppression of non-specific binding, which is a major challenge in biosensor technology. High surface density of oligosaccharides on material surfaces mimic glycocalyx-like structures and increase the surface area accessible to immobilized capture molecules (Löfas and Johnsson, 1990; Buckle et al. 1993; Brecht and Gauglitz 1995). A novel surface modification construct is presented: dextran, multiply substituted with photoactivatable groups (3-(trifluoromethyl)-3-(*m*-isothiocyanophenyl) diazirines), combines the properties of surface-passivating oligosaccharides and covalent cross-linker polymers (OptoDex) (Barié et al., 1998). The construction of optically homogeneous (molecular) layers of dextran – selectively applied at certain well-defined areas on the chip – was achieved by ink-jet printing and photobonding. OptoDex-coated waveguide sensor areas offer localized suppression of non-specific binding of biomolecules to waveguiding TiO_2 films. In the experiments, the dextran layers effected 4-fold up to 10-fold reduction of net binding of biotic fluid components at the time when specific biological interactions occurred. The biological fluids tested include detergent solubilized cow brain homogenate (8.3 mg/ml), artificial tear fluid containing 4.6 mg protein/ml and 0.076 mg lipid/ml, and undiluted human blood serum (Fig. 10 (a)).

The experiment shown in Fig. 10 was performed as follows: OptoDex was dissolved in diluted phosphate buffered saline (PBS, 1:100 in H_2O), and applied to one pad of the optical waveguide chip, here addressed as the sensor pad, by ink-jet printing. The other pad, the reference pad, was not treated. After drying under

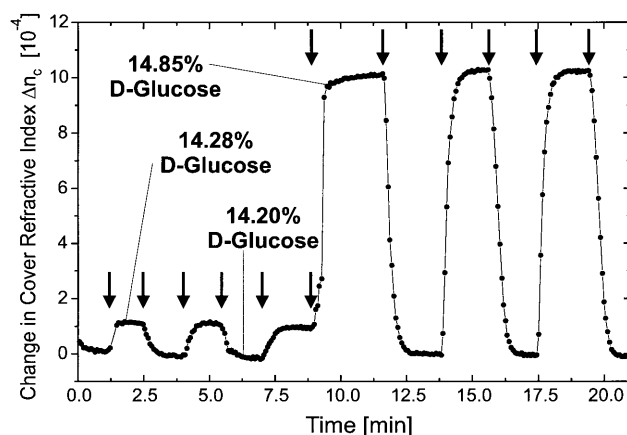


Fig. 9. CIOS system as refractometer.

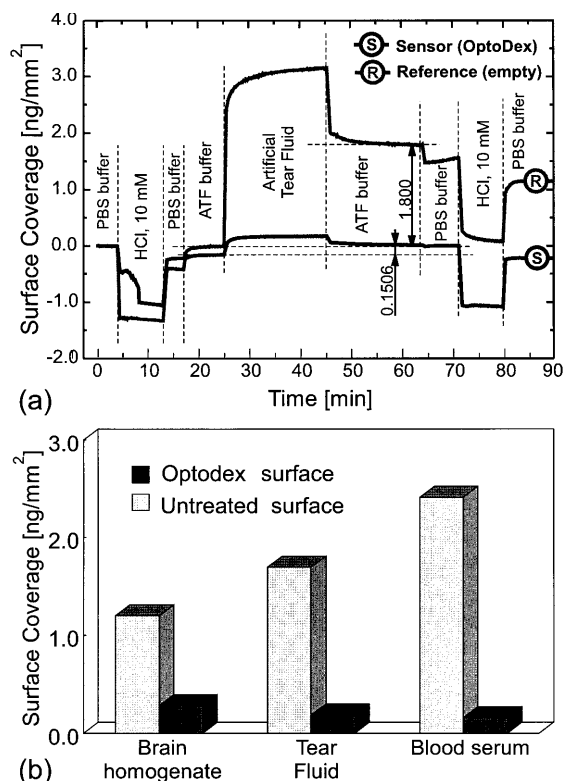


Fig. 10. On-line monitoring of interaction of artificial tear fluid constituents with material surfaces. (a) Dextran coating of the biosensor surface reduces adsorption of tear fluid constituents to TiO₂ and (b) surface passivation is equally shown with human blood serum and brain homogenate. Net values of adlayer surface density after washing are reported.

vacuum for 3 h, the chip was exposed to UV light for 4 min (Oriel Lamp, 350 nm wavelength, 11.0 mW/cm²). The chip was then washed with KSCN, 3.0 M (3 × 1.0 ml/chip), PBS containing 0.02% Tween 20 (3 × 1.0 ml/chip) and bidistilled water (3 × 1.0 ml/chip).

The interaction between biotic fluid constituents and sensor surface was on-line monitored. Exceptional suppression of biomolecule (adsorptive) binding was observed on the OptoDex pretreated pads, considering that the protein content of either fluid was heterogeneous and the protein concentration was > 4.6 mg/ml. The results unequivocally demonstrate that photo-bonded dextran efficiently suppresses biomolecule adsorption (Fig. 10(b)) even with undiluted samples.

9. Conclusions

The presented novel sensor system features a high functionality. It is suitable for accomplishing measurements of the effective refractive index with high resolution $\delta N \approx \pm 1.0 \times 10^{-6}$ for a wide range of applications with one single chip type. The operating

principle is based on moving a high-resolution measuring window over an extended measuring range. The high-resolution measuring window is realized by means of a CGC sensor for performing fast measurements with on-chip referencing, avoiding any mechanical movement during the measurement. The high-resolution window is placed to a desired working point by means of a variable angle of incidence of the readout laser beam. As an example, the described optical chips offer an operating range of $1.0 < n_c < 2.1$ for bulk refractometry. The reliability of the sensor system was enhanced by an in situ chip characterization procedure, which allowed correction for defects of the sensor chips or to reject chips not reaching the specifications. Important facts for practical applications are that the chips can be mass fabricated by replication techniques, and the properties of the high-resolution window can be chosen by the grating design. On-chip referencing was demonstrated by locally depositing an OptoDex layer for achieving suppression of non-specific binding.

Acknowledgements

We owe thank to I. Kjelberg and E. Meier for mechanical constructions, J.S. Pedersen for software, M.T. Gale, R. Müller, S. Westenhöfer and J. Söchtig for chip fabrication, J.-M. Moret, M. Liley, H. Sigrist and K. Knop for general support, T. Callenbach and K. Eggmann, Weidmann AG, Rapperswil, for collaboration on injection molding, and J. Edlinger and B. Maisenhölder, Unaxis Balzers Ltd., Balzers, Liechtenstein, for waveguide coating. Financial support by the KTI project MedTech/S_512 is also acknowledged.

References

- Barié, N., Rapp, M., Sigrist, H., Ache, H.J., 1998. Covalent photolinker-mediated immobilisation of an intermediate dextran layer to polymer coated surfaces for biosensing applications. *Biosensors Bioelectr.* 13, 885.
- Brandenburg, A., 1997. Differential refractometry by an integrated-optical Young interferometer. *Sensors Actuators B* 38–39, 266–271.
- A. Brecht, G. Gauglitz, 1995. Optical probes and transducers. *Biosensors Bioelectr.* pp. 923–936.
- Buckle, P.E., et al., 1993. The resonant mirror: a novel optical sensor for direct sensing of biomolecular interactions. Part II: applications. *Biosensors Bioelectr.* 8, 355–363.
- CRC Handbook of Chemistry and Physics, 70th ed. (1989). CRC Press, Boca Raton, pp. D221–D233.
- Cush, R., Cronin, J.M., Stewart, W.J., Maule, C.H., Molloy, J., Goddard, N.J., 1993. The resonant mirror: a novel optical biosensor for direct sensing of biomolecular interactions part I: principle of operation and associated instrumentation. *Biosensors Bioelectr.* 8, 347–364.
- Dübendorfer, J., Kunz, R.E., 1996. Reference pads for miniature integrated optical sensors. *Sensors Actuators B* 38–39, 116–121.

- Dübendorfer, J., Kunz, R.E., 1998. Compact integrated optical immunosensor using replicated chirped grating coupler sensor chips. *Appl. Opt.* 37, 1890–1894.
- Dübendorfer, J., Kunz, R.E., Jobst, G., Moser, I., Urban, G., 1998. Integrated optical pH sensor using replicated chirped grating coupler sensor chips. *Sensors Actuators B* 50, 210–219.
- Heideman, R.G., Kooyman, R.P.H., Greve, J., 1993. Performance of a highly sensitive optical waveguide Mach-Zehnder interferometer immunosensor. *Sensors Actuators B* 10, 209–217.
- Kempen, L.U., Kunz, R.E., 1994. Miniature integrated optical refractometer chip. *Proc. SPIE* 2208, 124–129.
- Karlsson, R., Stahlberg, R., 1995. Surface plasmon resonance detection and multispot sensing for direct monitoring of interactions involving low-molecular-weight analytes and for determination of low affinities. *Anal. Biochem.* 228, 274–288.
- Kubitschko, S., Spinke, J., et al., 1997. Sensitivity enhancement of optical immunosensors with nanoparticles. *Anal. Biochem.* 253, 112–122.
- Kunz, R.E., 1993. Gradient effective index waveguide sensors. *Sensors Actuators B* 11, 167–176.
- Kunz, R.E., Edlinger, J., Curtis, B.J., Gale, M.T., Kempen, L.U., Rudigier, H., Schütz, H., 1994. Grating couplers in tapered waveguides for integrated optical sensing. *Proc. SPIE* 2068, 313–325.
- Kunz, R.E., Edlinger, J., Sixt, P., Gale, M.T., 1995. Replicated chirped waveguide gratings for optical sensing applications. *Sensors Actuators A* 47, 482–486.
- Kunz, R.E., Dübendorfer, J., Morf, R.H., 1996. Finite grating depth effects for integrated optical sensors with high sensitivity. *Biosensors Bioelectr.* 11, 653–667.
- Kunz, R.E., 1999. Integrated optics in sensors: advances toward miniaturized systems for chemical and biochemical sensing. In: Murphy, E.J. (Ed.), *Integrated Optical Circuits and Components*. Marcel Dekker, New York.
- S. Löfas, B. Johnsson, 1990. A novel hydrogel matrix on gold surfaces in surface plasmon resonance sensors for fast and efficient covalent immobilization of ligands. *J. Chem. Soc., Chem. Commun.* 1526–1528.
- Lukosz, W., Stamm, Ch., Moser, H.R., Ryf, R., Dübendorfer, J., 1996. Difference interferometer with new phase-measurement method as integrated-optical refractometer, humidity- and biosensors. *Sensors Actuators B* 31, 203–207.
- T. Scheimpflug, 1904. British Patent GB 1196/1904.
- Schieber, P., Straub, J., 1990. Refractive index of water as function of wave, temperature and density. *J. Phys. Chem. Ref. Data* 19/3, 677–717.
- Tiefenthaler, K., Lukosz, W., 1984. Integrated optical humidity and gas sensors. *Proc. SPIE* 514, 215–218.